8th Thermal and Fluids Engineering Conference (TFEC)
May, 2023
Partially Online Virtual and at University of Maryland, MD Conference

TFEC-2023-45998

PUMPED, HYBRID TWO-PHASE COOLING SYSTEM FOR HIGH HEAT FLUX ELECTRONICS

Michael C. Ellis[1*], Elizabeth K. Seber[1], Mohammad Reza Shaeri[1]
Massoud Kaviany[2]

[1]Advanced Cooling Technologies, Inc., 1046 New Holland Avenue, Lancaster, PA 17601
[2]University of Michigan, Department of Mechanical Engineering, Ann Arbor, MI 48109

ABSTRACT

Advanced Cooling Technologies, Inc. (ACT) is developing an innovative hybrid two-phase cooling system (HTPCS) that combines the unique benefits of mechanically pumped two-phase systems with capillary-driven two-phase cooling. The HTPCS has several unique evaporator features that separate this system from traditional two-phase cooling systems. First, electronics are mounted to an Aluminum Nitride (AlN) plate that is in direct contact with a region that promotes thin film evaporation on the opposite side of each transistor. Mounting locations are provided using Direct Bond Copper (DBC) traces customized to the applications needs. This arrangement greatly reduces the thermal resistance between the electronics and coolant, which allows for high power and high heat flux management without a large temperature potential. By using a Kovar envelope to which the AlN is attached, all materials are Coefficient of Thermal Expansion (CTE) matched. This prevents stress at the joint between the electronics and evaporator as the electronics increase in temperature during operation. Inside the cold plate, a dielectric coolant, such as a refrigerant, enters through an inlet tube and is exposed to several capillary structures, or wicks. These structures pull liquid a short distance to a specially designed thin film evaporation surface. ACT demonstrated the removal of heat loads >300W/cm² while maintaining device temperatures below 80°C. The concept, design, and test data are discussed in this paper.

KEY WORDS: Two-phase, Evaporative Cooling, High Heat Flux, Electronics Cooling, Thin Film, Heat Transfer, Pumped Loop, Capillary

1. INTRODUCTION

Electronics' performance has made impressive gains in the past decade. Miniaturization and device integration have afforded these gains but also resulted in significant increases in power density. For instance, commercial server processors can reach heat fluxes over 100 W/cm^2 [1]. Advanced electronics such as high frequency communications arrays and High-Energy Laser (HEL) diodes can produce average heat fluxes exceeding 1,000 W/cm^2 [2, 3]. And with communications moving into higher frequency bandwidths like V- and W-bands [4, 5], HELs pushing 100's of kW's of delivered power [6], and increasing demand for more compact, higher power computing [1, 7], the upward trend for power dense and high heat flux electronics will continue. An example of this trend is shown in Fig. 1 for data center and

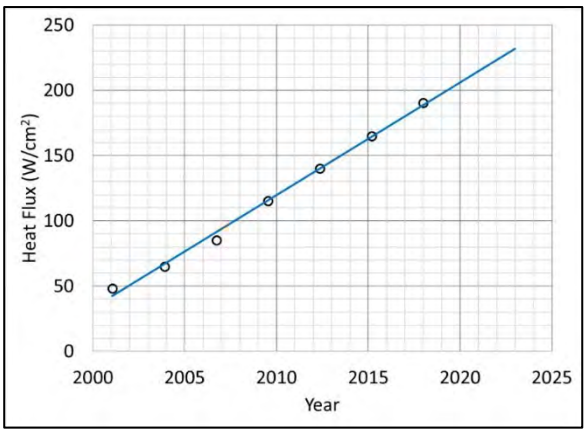

Fig. 1 Heat flux trend for data centers [7].

*Corresponding Author: mike.ellis@1-act.com

telecommunication electronics. This trend was generated from data collected during an industry-wide survey by The Uptime Institute and indicates that, by 2025, data center and telecommunication electronics that operate near 250 W/cm^2 could be commonplace. Laser diodes with power densities on the order of 10's of kW/cm^2 are expected to be a requirement for future HEL systems [8].

According to Newton's Law of Cooling and Fourier's Law, which describe convective and conductive heat transfer, respectively, an increase in heat flux results in an increase in the temperature potential required to transfer this heat. This occurs because system properties such as thermal conductivity, heat transfer coefficient, and heat transfer area do not change. So, if coolant temperature remains constant, the electronics temperature will increase until the heat generated by them can be rejected. There are some other effects not considered in this statement, such as temperature effects on material and fluid properties, the change in coolant outlet temperature for single-phase systems, and the effects of boiling regime on the heat transfer coefficient for two-phase systems, but is sufficient for understanding the effect of increasing heat flux on the temperature of the electronics.

While many modern electronics can handle temperatures up to 100 °C, operating at these temperatures greatly reduces the lifetime of the device. A general rule of thumb is that for every 10 °C that an integrated circuit operates over 25 °C, lifetime is halved [9]. Additional research has suggested that 15 °C is a more appropriate temperature metric but also identify thermal cycling as an additional concern with the potential to decrease lifetime by nearly a factor of 10 [10]. Compounding this problem is the method of ultimate heat rejection, which is typically to ambient temperatures. As a result, electronics have a relatively narrow operating temperature range.

With these temperature limitations, the only option to manage high heat flux electronics is improving the thermal resistances associated with conduction and convection. Conduction can be managed by minimizing the thickness and maximizing the thermal conductivity of substrate and heat sink materials. The goal of a good cold plate design should be to locate the heat source as close to the heat transport area as possible. Finally, the heat transport mechanism should maximize the convective heat transfer coefficient to rapidly remove heat to the ultimate sink.

2. HYBRID THERMAL MANAGEMENT CONCEPT

ACT has considerable experience in developing high heat flux thermal management devices that concentrate on bringing the heat source as close as possible to a heat transport mechanism with the highest possible convective heat transfer coefficient. Out of the many potential convective heat transfer processes, evaporative heat transfer can achieve heat transfer coefficients orders of magnitude greater than other approaches [11]. And of the evaporative processes, thin film evaporation provides the highest possible heat transfer coefficient. For instance, vapor chambers that rely on thin film evaporation have achieved heat transfer coefficients exceeding 200 kW/m^{2}K while operating at heat fluxes over 350 W/cm^2 and with an evaporator thermal resistance of 0.075 K/(W/cm^2). This level of performance was reached by using a monolayer wick fed by arterial wicks at the heat source [12, 13]. This wick is shown in Fig. 2.

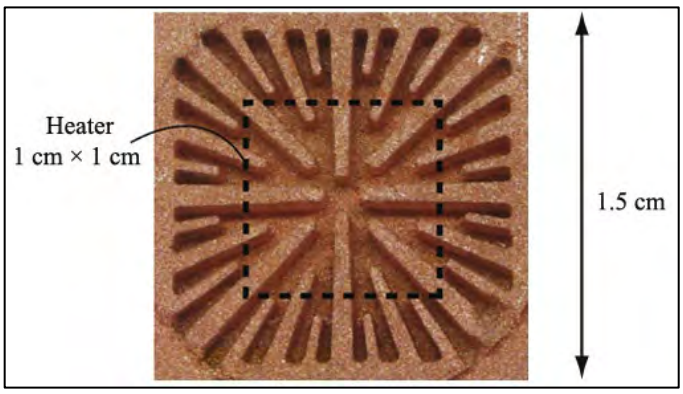

Fig. 2 Monolayer wick fed by arterial wicks. ACT was part of the team that developed these wicks [13].

Ideally, the entire heated surface would be covered by the monolayer wick. Since heat must be conducted from the heat source and through the liquid-saturated porous medium, a monolayer wick provides the lowest thermal resistance path to the evaporation surface. However, as with any two-phase heat transfer device, the limiting factor for maximum heat

flux is the Critical Heat Flux (CHF). In general, CHF occurs when liquid cannot return to the heated surface at a sufficient rate to support heat transfer solely by phase change. In a porous medium, such as the wick in a vapor chamber, this occurs when the pressure drop associated with the liquid flow rate required to support the evaporation rate overcomes the capillary capability of the wick. As CHF is approached, the meniscus in the porous medium retreats from the evaporation surface until finally only vapor is present and dry out occurs. And, while a monolayer wick provides minimal thermal resistance, the low profile, and typically smaller pore size, results in much higher liquid pressure drop and, in effect, constricts liquid return to the heated surface.

The purpose of the arterial wicks is to provide a low pressure drop liquid return path to the heated surface, at the cost of low thermal resistance evaporation area. As such, there exist optimal designs that maximize the return provided by a monolayer wick fed by arterial wicks. This optimization process is discussed in detail in the work by Hwang et al [13].

In addition to moving through the wick at the evaporator, or heat input, surface, liquid must also travel back through a porous structure from the cooled, or heat output, surface of the vapor chamber. Consider the basic vapor chamber design, shown in Fig. 3. Vapor chambers are heat spreaders and, the higher the heat flux, the larger the heat output surface needs to be. As a result, the liquid return path can be significant. And, since liquid transport is accomplished by capillary means, sufficiently small pore sizes are required. Together, these factors can result in significant liquid return pressure drop and further reduce the maximum heat flux that can be achieved before CHF is reached.

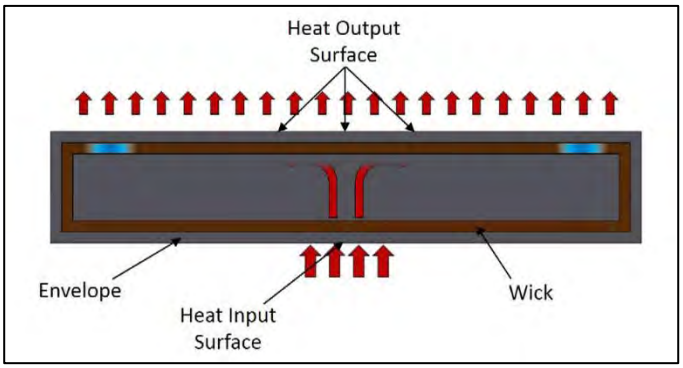

Fig. 3 Basic vapor chamber liquid and vapor flow path between the heat input and output surfaces.

Eliminating the liquid return pressure drop was the primary goal of the Hybrid Two-phase Cooling System (HTPCS) concept developed by ACT [14]. This concept, shown in Fig. 4, relies on an actively pumped liquid supply rather than a capillary-driven one. When the liquid flow channel is properly designed, this arrangement allows for liquid to be supplied at a high flow rate and low pressure drop to the wicks, which then pull liquid to the heat surface. Then, arterial-fed, monolayer wicks can be used at the heated surface to maximum heat transfer rate. The wicks provide another function: separation of the liquid and vapor phases. The liquid flow path is physically separated from the vapor region. Liquid can only enter through the porous medium. And the path from the liquid channel to the heat source can be minimized to almost negligible distances. As a result, the cold plate allows for high liquid flow delivery while still providing a region for film evaporation. This is the hybrid nature of this design and combines the benefits of a pumped two-phase system with the high heat transfer performance of a vapor chamber.

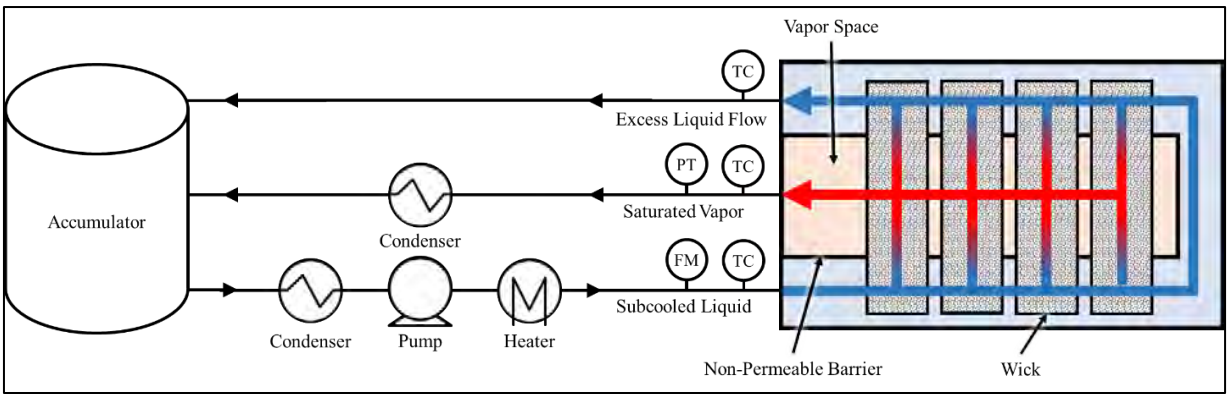

Fig. 4 Hybrid Two-Phase Cooling System (HTPCS) concept.

3. APPLICATION

ACT originally developed the HTPCS to address the needs of an experiment being conducted at Fermilab. This experiment relied on 8 high frequency (>100 GHz) Gallium Nitride (GaN) transistors located in close proximity to each other. This led to three challenges: maintain the transistor junction temperature below 90 °C while managing high heat fluxes (>300 W/cm^2), prevent thermal stress at the junction by using materials that matched the Coefficient of Thermal Expansion (CTE) of the GaN transistors, and provide electrical isolation to prevent parasitic capacitance losses. The location of the transistors, four in a linear pattern on each side of the cold plate, and the need for a remote heat sink several meters from the cold plate also impacted the design.

4. PROTOTYPE DESIGN AND FABRICATION

The HTPCS has several unique evaporator features that separate this system from traditional two-phase cooling systems. As shown in Fig. 5, electronics are mounted to an Aluminum Nitride (AlN) plate that is in direct contact with a region that promotes thin film evaporation on the opposite side of each transistor. Thin film evaporation is one of the most effective heat transfer mechanisms and is capable of reaching heat transfer coefficients greater than 100,000 W/cm^2. Mounting locations are provided using Direct Bond Copper (DBC) traces customized to the applications needs. This arrangement greatly reduces the thermal resistance between the electronics and coolant, which allows for high power and high heat flux management without a large temperature potential, while the AlN provides electrical isolation between the electronics to prevent losses from parasitic capacitance. By using a Kovar envelope to which the AlN is attached, all materials are Coefficient of Thermal Expansion (CTE) matched. This prevents stress at the joint between the electronics and evaporator as the electronics increase in temperature during operation. Stress at this joint can cause the solder joint to fail and, in turn, the electronics to become detached from the cold plate, which results in electronics overheating and failure. Inside the cold plate, a dielectric coolant, such as a refrigerant, enters through an inlet tube and is exposed to several capillary structures, or wicks. These structures pull liquid a short distance to a specially designed thin film evaporation surface. Here the refrigerant changes phases and exits the device, carrying away heat as latent heat. Liquid is quickly resupplied to the heated surface and high heat transfer rates are achieved. ACT demonstrated the removal of heat loads >300W/cm² while maintaining device temperatures below 80°C (10 °C lower than Fermilab's 90 °C requirements). Heat transfer coefficients of 60,000 W/m²K and greater were achieved, which is considerably higher compared to typical refrigerant-based pumped two-phase cooling systems.

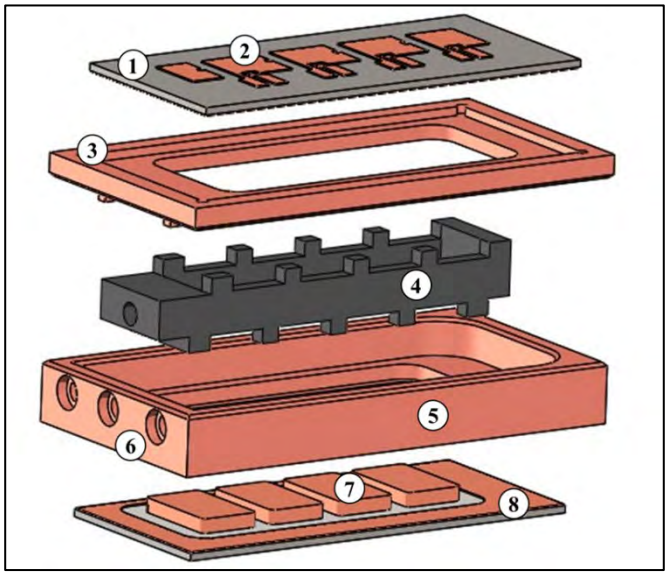

Fig. 5 Compact hybrid evaporator with the following labeled components 1.) AlN Plate, 2.) Direct-bond copper trace for transistors which are present on the topside of both AlN plates, 3.) Copper-coated Kovar ring, bottom-side, 4.) Rubber non-permeable barrier, 5.) Copper-coated Kovar ring, topside, 6.) Liquid and vapor inlet/outlet, 7.) Sintered wicks, which are present on the underside of both AlN plates, 8.) Direct-bond copper trace for joining AlN Plates to Kovar rings

The hybrid cold plate, shown in Fig. 6, is a hermetically sealed and compact enclosure where heat is removed from transistors through capillary evaporation. The cold plate was fabricated by brazing two Direct Bonded Copper (DBC) Aluminum Nitride (AlN) substrates to a Kovar ring, which is CTE-matched and have a low CTE of around 5.5 ppm/K and 5.9 ppm/K, respectively. Also, DBC/AlN is CTE-Matched with GaN, which allows direct soldering of the GaN chip to the cold plate. Compared with printed circuit boards, DBC ceramic

substrates exhibited four times lower thermal resistance, and significant mitigation of parasitic inductance. In addition, AlN has a relatively high thermal conductivity (150-200 W/m-K) compared with the low thermal conductivity of PCB materials (typically FR4 < 1 W/m-K). The DBC layers allow for the sintering of the wick structures on the evaporators, as well as direct soldering of GaN transistors on the external surface of the substrates. Fig. 7 shows an x-ray of one half of the assembled evaporator, highlighting how the arterial wick aligns with the DBC trace defined by Fermilab. A DBC trace was also added to the edge of the AlN plate to aid in brazing to the Kovar ring.

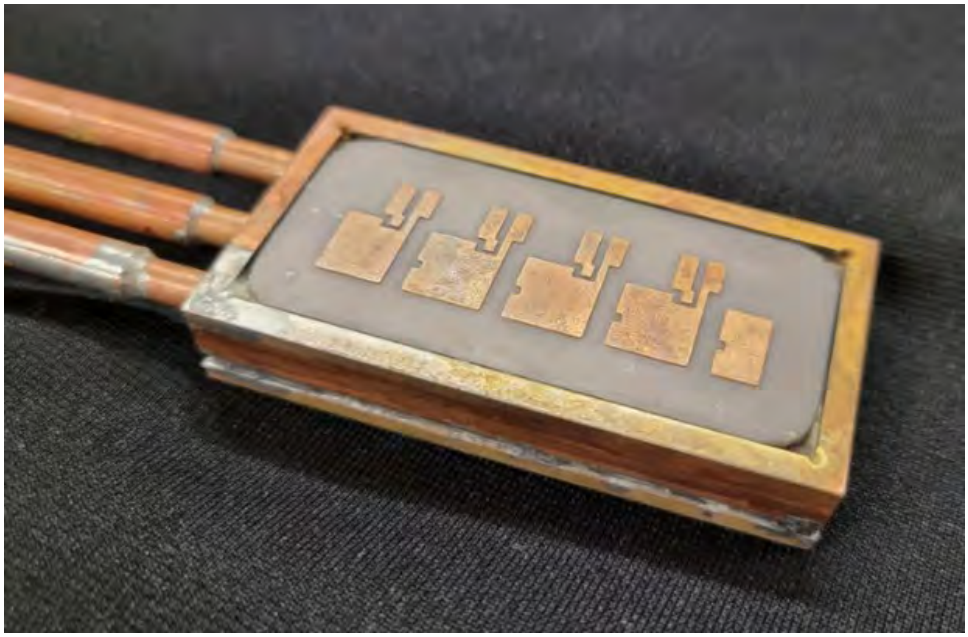

Fig. 6 Fabricated, AlN hybrid two-phase cold plate

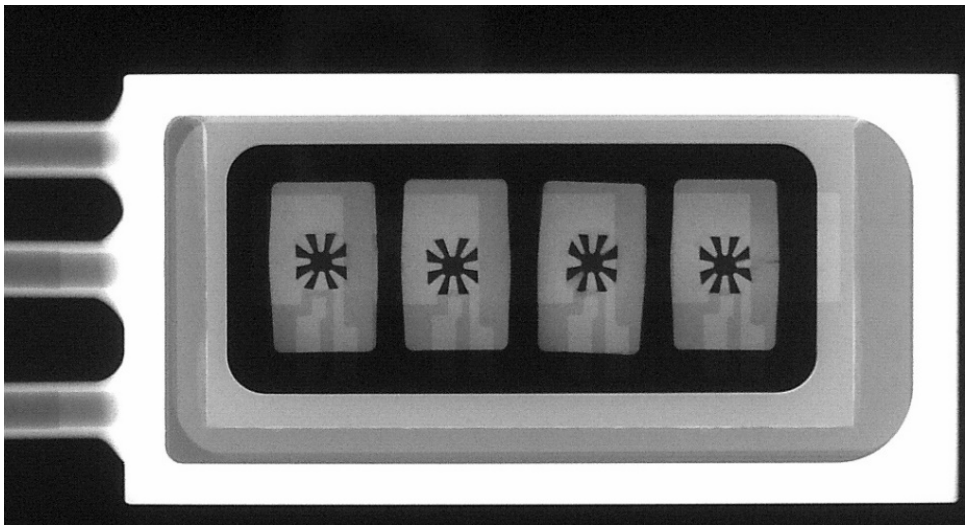

Fig. 7 X-Ray image of assembled Kovar ring, top half

Heat generated by the individual transistors is conducted via the AlN substrates of the cold plate and absorbed through the wick evaporators. The mechanical pump continuously supplies liquid to the cold plate and wicks. The remaining liquid that is not absorbed by the capillary action of the wicks is excess flow. To prevent large thermal resistances resulting from flooded wicks by liquid, the evaporators are separated by a thin dielectric housing seal, called a Non-Permeable Barrier (NPB). As a result, the interior space of the NPB contains only vapor, and the exterior space is a two-phase mixture. Since the pressure inside the separator is higher than that on the exterior side, liquid cannot penetrate the NPB and enter the vapor space. Moreover, the separator allows

the excess flow to turn inside the cold plate (from the gap between the separator and the ring's wall) and exit the cold plate from the same side of the inlet manifold, which was a Fermilab requirement.

The system design of the HTPCS test system is shown in Fig. 8. Liquid refrigerant stored in the accumulator is pumped through a subcooling condenser to prevent cavitation in the pump. Following this, the liquid is pumped through the hybrid cold plate, where saturated vapor is generated in the wick structure and excess liquid is pumped through the system. Both lines are sent back to the accumulator, where the vapor is first cooled by a condenser to a subcooled liquid. The cycle then continues. A series of temperature and pressure probes are placed throughout the system to map the conditions of the working fluid. Valves are placed at strategic locations to assist in flow control. One such valve is a back-pressure regulator, placed on the vapor excess line, to control the vapor pressure. This allows for control of the saturation pressure within the vapor space.

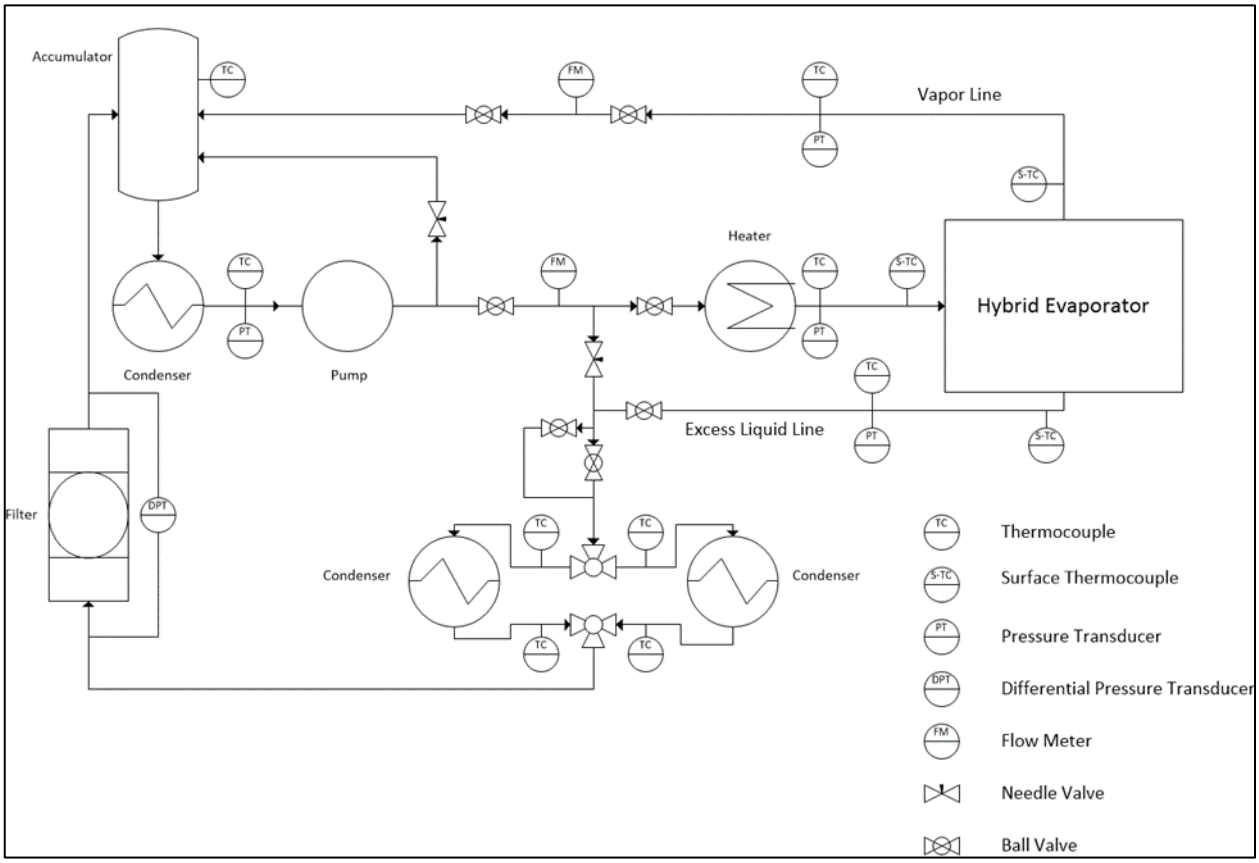

Fig. 8 HTPCS test process flow diagram

5. TEST RESULTS

Fig. 9 shows the temperature profile of the top and bottom plates for a single representative test of the hybrid cold plate prototype. The top plate, which holds Heat Sources 1-4, provides nearly isothermal operation until the heat flux reaches just over 250 W/cm². The temperatures of the heat sources separate here, indicating that some of the wicks may be experiencing dry out at this increased heat load. Looking at the bottom plate, we see a spread in the temperatures of the different heat sources from the onset of testing. This is indicative of differing thermal resistances between these heat sources which could be the result of different attachment conditions. Overall, we see that the bottom plate operates at temperatures lower than the top plate, likely a result of the bottom plate being gravity aided. Overall, the device performed as intended with junction temperatures staying below the 90 °C limit when operating at 300 W/cm².

The heat transfer coefficient (HTC), calculated from the temperature and power data, for each heat source is shown in Fig. 10. As heat flux increases from zero, we see the HTC for each plate increase before leveling off as normal operation occurs. During normal operation, we can see that the HTC rests comfortably around 50,000 W/m²K for the top plate, and between 55,000-60,000 W/m²K for the bottom plate. For the top plate, the HTC diverges after 250 W/cm^2, indicating the possibility of dry out in some of the wicks. Overall, this is a rather high value, as typical refrigerant-based cooling systems see an HTC of around 10,000 W/m²K.

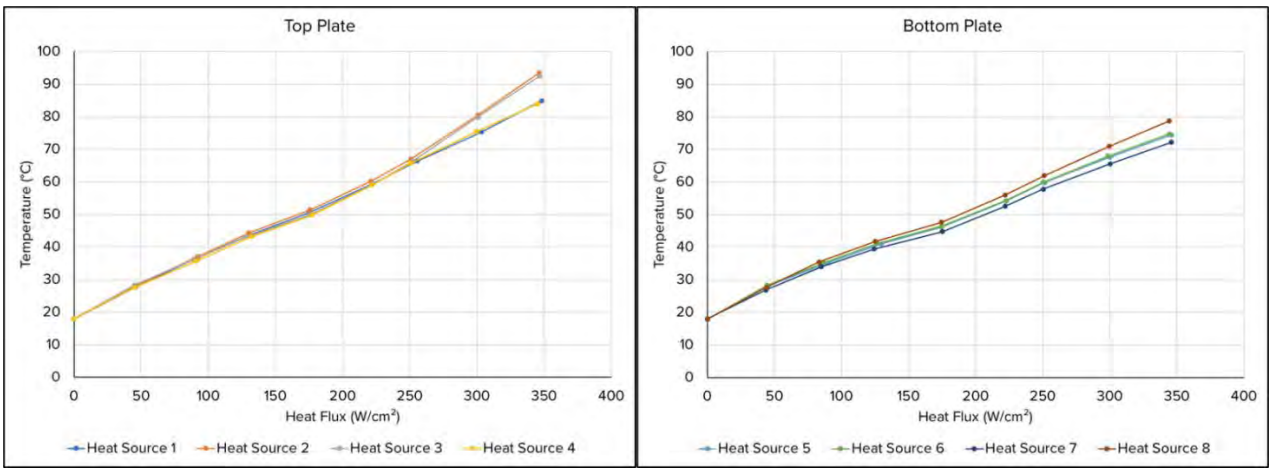

Fig. 9 Temperature results on the top and bottom plates of the hybrid two-phase cold plate for varying heat flux

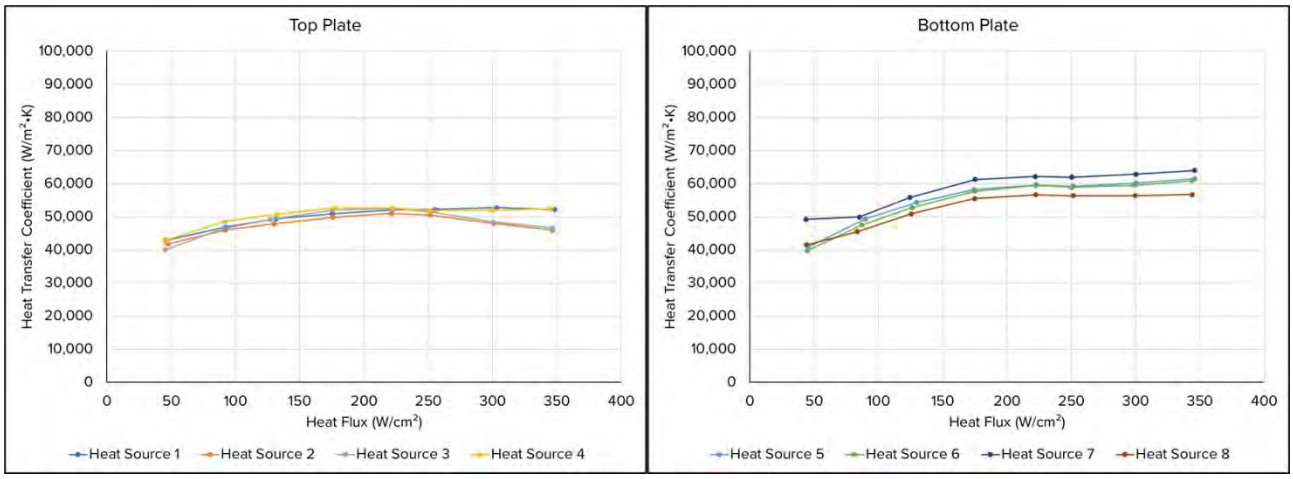

Fig. 10 Heat transfer coefficient for the top and bottom plates of the hybrid two-phase cold plate for varying heat flux.

6. CONCLUSIONS

ACT developed a dielectric, hybrid, pumped two-phase cooling system that maintained heat sources at temperatures lower than 90 °C while operating at heat fluxes over 300 W/cm², achieving heat transfer coefficients as high as 60,000 W/m²K, minimizing parasitic capacitance through a dielectric design, and providing a CTE-matched cooling surface that allowed the GaN transistors to be directly mounted to the cold plate. ACT is currently extending development of the HTPCS beyond the Fermilab application to power electronics, HEL systems, and high frequency communication systems. This work, funded by the Department of Energy (DOE) and the Department of Defense (DOD), will seek to improve on the Fermilab design to achieve higher heat flux capability, optimize the manufacturing process, and minimize the chip-to-coolant thermal resistance. Currently, efforts are underway to bring the coolant closer to the heat rejection surface and

improve the artery-fed, monolayer wick design. In addition, new additive manufacturing techniques, such as printing variable porosity wick structures, are being investigated for this cold plate design.

ACKNOWLEDGEMENT

The authors would like to think Dr. John Boger at DOE for funding this work through the Small Business Innovation Research (SBIR) program. We would also like to recognize the efforts of our technical team at ACT, including Max Demydovych, Larry Waltman, Aryiannah McGee, Phil Martin, and Adam Shreve.
references

[1] C. De Castro and S. Murshed, "A critical review of traditional and emerging techniques and fluids for electronics cooling," *Renewable and Sustainable Energy Reviews,* vol. 78, pp. 821-833, 2017.

[2] R. Warzoha, A. Wilson, B. Donovan, N. Donmezer, A. Giri, P. Hopkins, S. Choi, D. Pahinkar, J. Shi, S. Graham, Z. Tian and L. Ruppalt, "Applications and Impacts of Nanoscale Thermal Transport in Electronics Packaging," *Journal of Electronics Packaging,* vol. 143, no. 2, 020804, pp. 1-29, 2021.

[3] J. Skidmore, B. Freitas, J. Crawford, J. Satariano, E. Utterback, L. DiMercurio, K. Cutter and S. Sutton, "Silicon monolithic microchannel-cooled laser diode array," *Applied Physics Letters,* vol. 77, pp. 10-12, 2000.

[4] Federal Communications Commission, "FCC Grants SpaceX NGSO V-band Authorization," FCC 18-161, 2018.

[5] Federal Comnnuications Commision, "FCC Grants Boeing NGSO V-band Authorization," FCC 21-115, 2021.

[6] J. Rothenberg, "Compact High Energy Laser Engineering Assessment (CHELSEA)," AFRL-RD-PSTR-2020-0029, 2020.

[7] The Uptime Institute, "Heat density trends in data processing, computer systems and telecommunication equipment," 2018.

[8] C. Häfner, C. Holly, H. Hoffmann, L. Gruber, M. Crowley, L. Woods, R. Walker, P. Thiagarajan, S. McDougall, K. Boucke, G. Lui, G. Lui, J. Jandeleit, A. Zeitschel, R. Hülsewede and R. Deri, "Status and perspectives of high-power pump diodes for inertial fusion energy lasers," in *IFE Science & Technology Community Strategic Planning Workshop,* Virtual, 2022.

[9] R. Wilcoxon, "Advanced cooling techniques and thermal design procedures for airborne electronic equipment - revisited," in *IMAPS Thermal Management Advanced Technology Workshop,* Los Gatos, CA, 2016.

[10] Department of Defense, "Reliability prediction of electronic equipment," MIL-HDBK-217F, 1991.

[11] Z. Zhang, X. Wang and Y. Yan, "A review of the state-of-the-art in electronic cooling," *Advances in Electrical Engineering, Electronics, and Energy,* Vols. 1, 100009, pp. 1-26, 2021.

[12] Y. Sungtaek Ju, M. Kaviany, Y. Nam, S. Sharratt, G. Hwang, I. Catton, E. Fleming and P. Dussinger, "Planar vapor chamber with hybrid evaporator wicks for thermal management of high-heat-flux and high-power optoelectronic devices," *International Journal of Heat and Mass Transfer,* vol. 60, pp. 163-169, 2013.

[13] G. Hwang, E. Fleming, B. Carne, S. Sharratt, Y. Nam, P. Dussinger, Y. Ju and M. Kaviany, "Multi-artery heat-pipe spreader: Lateral liquid supply," *International Journal of Heat and Mass Transfer,* vol. 54, pp. 2334-2340, 2011.

[14] M. Reza Shaeri, R. Bonner, M. Ellis, E. Seber and M. Demydovych, "Heat Transfer Device Having an Enclosure and a Non-permeable Barrier Inside the Enclosure," U.S. Patent No. 11,408,683, 2020.